Increasing frequency, intensity and duration of observed global heatwaves and warm spells

S. E. Perkins,[1] L. V. Alexander,[1] and J. R. Nairn[2]

Received 31 July 2012; revised 25 September 2012; accepted 27 September 2012; published 27 October 2012.

[1] Using the latest HadGHCND daily temperature dataset, global trends in observed summertime heatwaves and annually calculated warm spells for 1950–2011 are analysed via a multi-index, multi-aspect framework. Three indices that separately focus on maximum temperature (TX90pct), minimum temperature (TN90pct) and average temperature (EHF) were studied with respect to five characteristics of event intensity, frequency and duration. Despite which index is employed, increases in heatwave/warm spell intensity, frequency and duration are found. Furthermore, TX90pct and TN90pct trends are larger and exhibit more significance for warm spells, implying that non-summer events are driving annual trends over some regions. Larger increases in TN90pct aspects relative to EHF and TX90pct are also observed. While qualitative information on event trends is similar across the indices, quantitative values vary. This result highlights the importance of employing the most appropriate index when assessing the impact of sustained extreme temperature events.
Citation: Perkins, S. E., L. V. Alexander, and J. R. Nairn (2012), Increasing frequency, intensity and duration of observed global heatwaves and warm spells, *Geophys. Res. Lett.*, *39*, L20714, doi:10.1029/2012GL053361.

1. Introduction

[2] In the absence of a universal definition, heatwaves are broadly defined as a period of consecutive days where conditions are hotter than normal, thereby including seasonally extreme (i.e. summertime) events, or seasonally anomalous warm spells (i.e., annual). During the last decade, a suite of severe heat waves have occurred over various global regions [*Trigo et al.*, 2005; *Karoly*, 2009; *Barriopedro et al.*, 2011]. Impacts of heatwaves include increased rates of human mortality; strains on man-made infrastructure; and increased rates and intensities of wildfires, which have devastating effects on both the natural and built environment [*Coumou and Rahmstorf*, 2012]. The global interest in heatwaves over a wide range of sectors is therefore not surprising, however it is this expansive interest that is responsible for the lack of common metric/s used to quantify such events.

[3] Indices used for heatwave or warm spell measurement may involve either percentile or fixed thresholds, include maximum, minimum or apparent temperature, and may focus on either consecutive days where conditions above the threshold persist or single daily events [e.g., *Meehl and Tebaldi*, 2004; *Alexander et al.*, 2006]. Such metrics may vary in complexity, ranging from numerous pre-defined conditions to be satisfied [e.g., *Meehl and Tebaldi*, 2004] or meticulous calculations of apparent temperature [e.g., *Fischer and Shär*, 2010], to simple counts of single days above a prescribed threshold [e.g., *Fischer et al.*, 2011].

[4] Based on a variety of indices described above, a handful of modeling studies have projected global increases in heatwave and warm spell intensity, frequency and duration over the next century [e.g., *Clark et al.*, 2006] and large Northern Hemisphere [e.g., *Meehl and Tebaldi*, 2004] and Southern Hemisphere [e.g., *Alexander and Arblaster*, 2009] regions. When considering observed heatwaves and warm spells, results are less coherent, which inhibits the ability to draw comprehensive conclusions in recent changes, as well as having confidence in future projections. This is due to many reasons, including single-event or region-specific studies [e.g., *Barriopedro et al.*, 2011], the surplus of indices employed, or the observational data set and temporal length considered. For temperature extremes in general, most global regions show larger increases in minimum temperature than maximum temperature [*Alexander et al.*, 2006; *Donat and Alexander*, 2012], however global changes in consecutive days of extreme temperature remain unclear.

[5] The aim of this study is to assess whether "global" conclusions can be drawn regarding changes in observed heatwaves and warm spells. In order to obtain consistent global trends of observed events, we employ a daily global temperature dataset and focus on the event intensity, frequency and duration as measured using three heatwave indices, Section 2 describes the data and methods, Section 3 presents our results and Section 4 provides the discussion and main conclusions of this study.

2. Data and Methods

[6] The HadGHCND data set provides gridded daily land-based values of maximum (T_{max}) and minimum temperature (T_{min}) [*Caesar et al.*, 2006; *Donat and Alexander*, 2012] for a large area of the globe (mostly mid- to high-latitude areas). Input station data are interpolated onto a 3.75° × 2.5° longitude/latitude grid, with a process that removes much of the inconsistency present in global station observations. The latest version of HadGHCND extends from 1950–2011, inclusive. Each grid point was considered for analysis providing it had data for at least 60% of the 62-year period and at least 5% of data between 2000–2011. This allows for event calculation over the equivalent of 39 years of data, as well as ensuring that the last decade is represented – not all areas covered by HadGHCND have sufficient data after 2000.

[1]Centre of Excellence for Climate System Science, Climate Change Research Centre, University of New South Wales, Sydney, New South Wales, Australia.
[2]Australian Bureau of Meteorology, Kent Town, South Australia, Australia.

Corresponding author: S. E. Perkins, Centre of Excellence for Climate System Science, Climate Change Research Centre, University of New South Wales, Sydney, NSW 2052, Australia. (sarah.perkins@unsw.edu.au)

0094-8276/12/2012GL053361

Higher thresholds were explored however this minimized data coverage much more so than trend robustness.

[7] Three indices were calculated for warm spells (anomalously warm periods over the entire year), and heatwaves (anomalously warm periods over a 5-month summer). The boreal (austral) summer extends from May-September (November-March). These indices include:

[8] 1. TX90pct (TN90pct), where the threshold is the calendar day 90th percentile, based on a 15-day window for T_{max} (T_{min}) [e.g., *Fischer and Shär*, 2010]; and

[9] 2. EHF, the excess heat factor (see auxiliary material) (J. Nairn and R. Fawcett, Defining heatwaves: Heatwave defined as a heat-impact even servicing all community and business sectors in Australia, manuscript in preparation, 2012), where heatwave conditions exist when EHF > 0.[1]

[10] For each index, a heatwave/warm spell is defined when the respective threshold is exceeded for at least three consecutive days [*Pezza et al.*, 2012]. TX90pct (TN90pct) represents daytime (nighttime) heat waves, whereas EHF is based on average daily temperature.

[11] Further to the three indices, we use a multi-aspect framework, where various attributes of heatwave frequency, intensity and duration are represented. The framework was based on that of *Fischer and Shär* [2010], who focus on:

[12] 1. HWN – the total number of events;

[13] 2. HWD – the length of the longest event;

[14] 3. HWF – the total number of days satisfying index criteria; and

[15] 4. HWA – the hottest day (amplitude) of the hottest event.

[16] We also include HWM - the mean event intensity, calculated by averaging all participating event days. Here we mainly focus on spatial trends of HWF and HWA, and globally averaged time series and trends for HWD and HWA, although global averages of all trends per index and aspect are briefly discussed. Due to different seasonal lengths, HWF (HWN) were converted to relative terms, such that HWF (HWN) reflects the percentage of days (monthly occurrences) per annual heatwave/warm spell. This was computed by dividing HWF (HWN) values by the number of days (months) within the season, i.e. 151 and 153 days (5 months) for boreal and austral summertime heat waves, respectively, and 365 days (12 months) for warm spells; and multiplying the result by 100. Using the non-parametric Kendall's slope estimator [*Sen*, 1968; *Zhang et al.*, 2005], trends per decade were calculated for each grid box where at least 20 years of heatwave metrics were observed. Statistical significance was computed at the 5% level.

3. Results

[17] Observed trends in percentage of days per season (HWF) for each index are mostly increasing for both warm spells and heat waves (Figure 1). For HWF(TX90pct) and HWF(TN90pct), trends are slightly larger in magnitude and exhibit greater statistical significance during warm spell events (1a, 1d) than during heatwaves (1b, 1e). Over much of Northern America, Eurasia and Australia warm spell HWF(TX90pct) and HWF(TN90pct) trends are at least 0.9%/decade, however mostly exceed 1.2%/decade. Heatwave trends of HWF(TX90pct) and HWF(TN90pct) bear similar magnitudes and areas of statistical significance, however are confined to coastal areas of Northern America, Northeast and Central Eurasia, and Southern Australia. Warm spell HWF (TN90pct) are slightly larger in magnitude than HWF (TX90pct) over central America and eastern Eurasia.

[18] Observed HWF(EHF) trends are smaller for warm spell (1g) than heatwave (1h) events. This is likely due to the index's reference to a climatological threshold, such that anomalous conditions generally only exist during periods of warm temperature, thereby reducing the possibility of anomalously warm events occurring outside summer (see auxiliary material). While summertime heatwave days (i.e. HWF) contribute to annual warm spell days, their weighting is reduced. Compared to HWF(TX90pct) and HWF (TN90pct) warm spells, HWF(EHF) trends are smaller in magnitude and display less significance. Increasing significant trends between 0.6–0.9%/decade exist for northern America, central Asia and southern and eastern Australia. Slightly higher trends of up to 1.5%/decade occur over western Europe and western Asia. Heatwave HWF(EHF) trends (1h) display similar significance to respective warm spell trends, however magnitudes are generally 0.9%–1.2% higher.

[19] Figure 1 also presents warm spell trends in peak of the hottest event (HWA) per index. Summer heatwave trends are not shown since the pattern and significance is very similar, albeit smaller in magnitude for some areas. Similar to HWF (TN90pct), HWA(TN90pct) trends (1f) are larger in magnitude than HWA(TX90pct). Increasing significant trends of up to 2°C/decade occur over northeast and southeast Asia, and 0.8–1°C/decade over Europe, northwest Canada and coastal U.S.A. Non-significant increasing trends also exist for Australia and southeast South America. HWA(TX90pct) trends (1c) exhibit similar statistical significance to HWA (TN90pct), although are generally 0.4–0.8°C smaller in magnitude.

[20] Observed trends of HWA(EHF) (1i) exhibit less statistical significance than HWA(TX90pct) and HWA (TN90pct). Higher trend magnitudes compared to HWA (TX90pct) and HWA(TN90pct) are due to the units, which consider the *excess* heat impact during an event and are in $^{\circ}C^2$ (see auxiliary material). Regions that display increases in HWA(TN90pct) and HWA(TX90pct) heatwaves also exhibit increases in HWA(EHF) amplitudes. In particular, significantly increasing trends over northeast and southwest Eurasia (2.4–2.7 and 0.6–0.9 EHF units/decade, respectively), and eastern and western Europe (2.4–2.7 EHF units/decade). Areas of non-significant decreasing HWA(EHF) trends correlate with areas of decreasing trends and/or little change based on HWA(TX90pct) and HWA(TN90pct).

[21] Figure 2 displays globally averaged time series and trends for warm spell event length (HWD) and peak of the hottest event (HWA). All three indices show increasing trends for both aspects, however yearly values and trend magnitude vary. For example, HWD(EHF) consistently shows the longest duration and the largest respective trend (see Table 1). When considering event peak, HWA (TX90pct) exhibits larger event magnitudes, while HWA (TN90pct) exhibits the largest trend (see Table 1). Although specific yearly magnitudes and rates of change are different, the time series pattern is similar among the three indices. For example, all indices measure very long and intense events for

[1] Auxiliary materials are available in the HTML. doi:10.1029/2012GL053361.

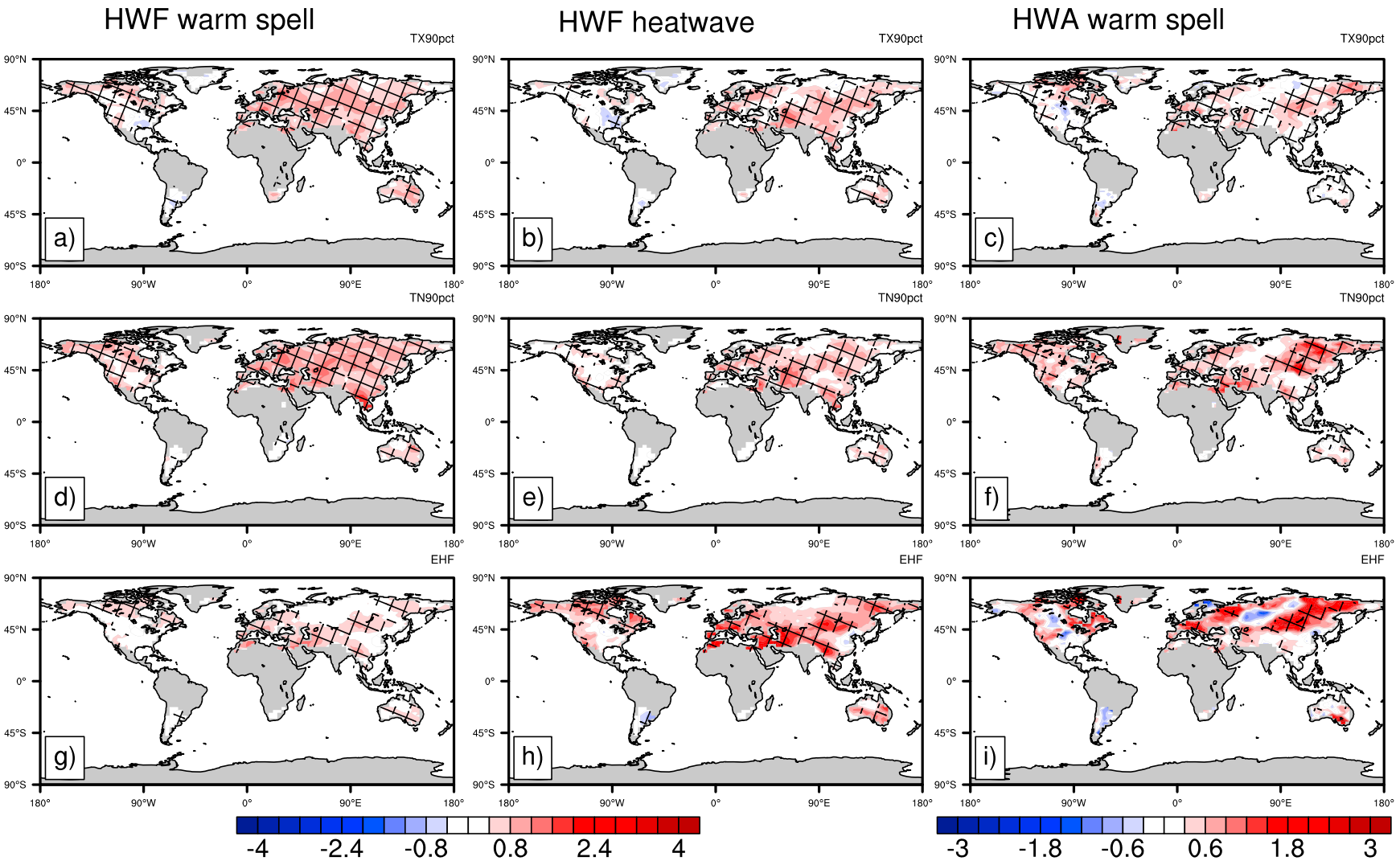

Figure 1. (left) Warm spell and (middle) heatwave trends in the number of days participating in an event (HWF), in which conditions persist for at least three consecutive days; and (right) warm spell trends in the peak of the hottest event (HWA). Indices include (a, b, c) TX90pct, (d, e, f) TN90pct and (g, h, i) EHF. Trends are for the period 1950–2011, computed by the non-parametric Kendall slope estimator [*Sen*, 1968]. Units are percentage of days per season/decade for the left and middle columns. Units for the right column are °C/decade for TX90pct and TN90pct, and $°C^2$/decade for EHF. Hatching represents where trends are significant at the 5% level, and grey indicates areas where there are insufficient observations for this study.

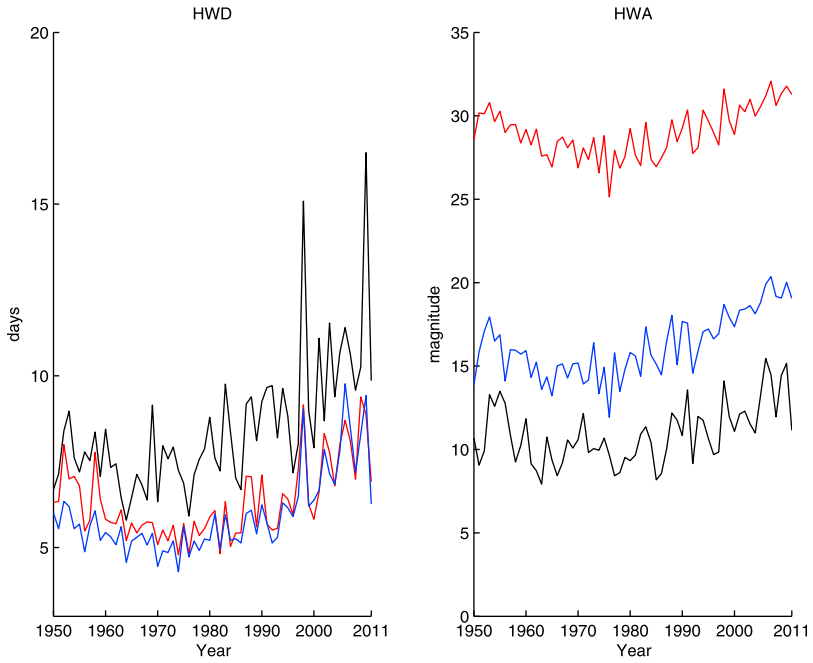

Figure 2. Annual globally averaged warm spell time series of (left) HWD (event length) and (right) HWA (peak magnitude of hottest event) for TX90pct (red), TN90pct (blue) and EHF (black). HWD units are average days/year, and HWA units are °C for TX90pct and TN90pct, and EHF (°C^2; excess heat) units for EHF. See Table 1 for corresponding trends.

1998 and 2010; the years of a very strong El Niño, and the spatially extensive and prolonged Russian heat wave. Indeed, trends over Eurasia in Figure 1 and globally averaged time series in Figure 2 may appear quite different if analysis was truncated at 2009.

[22] Globally averaged trends for all indices and aspects (Table 1) highlights that TN90pct exhibits the largest trends for most aspects when considering (annual) warm spells. This means that warm spells based on T_{min} only are showing greater rates of increase than those based on T_{max} and average temperature. Interestingly, this result is not consistent for (summertime) heatwaves, where trends of EHF are largest for the event length (HWD), percentage of participating days (HWF) and peak of the hottest event (HWA). Table 1 also demonstrates that considerably larger trends exist for warm spells than heatwaves for all indices. HWF exhibits the largest trends, which influences increases in HWD and the number of events (HWN).

4. Discussion and Conclusions

[23] The present study analyses observed global trends in warm spells and heat waves from 1950–2011. Three indices are employed using a multi-aspect framework, such that results are applicable to many different sectors, and that changes in numerous attributes of heatwaves and warm spells are ascertained. We find that, at the global scale, increases in warm spell and heatwave frequency, intensity and duration have occurred. This is clearly demonstrated through decadal trends based on three indices of the percentage of participating days (HWF, Figure 1), magnitude of the hottest day of the hottest event (HWA, Figures 1 and 2) and event length (HWD, Figure 2).

[24] Significantly increasing trends for HWF(TX90pct) and HWF(TN90pct) warm spells occur over a larger area and show slightly higher magnitudes than respective heatwaves. This result is interesting; heatwaves are generally regarded as a summertime phenomenon [e.g., *Barriopedro et al.*, 2011], yet our results for these two indices suggest warm spells (i.e. non-seasonal heatwaves) may drive annual trends more so than summertime heatwaves over some regions. The opposite heatwave/warm spell pattern is observed for HWF(EHF), which is likely due to impact orientation of the index, such that most events are detected during summer (see auxiliary material).

[25] Trends in nighttime (TN90pct) events are mostly larger than daytime (TX90pct) and combined (EHF) events. The relationship between TN90pct and TX90pct trends is consistent with global trends of non-consecutive extreme T_{min} and T_{max} events [*Vose et al.*, 2005; *Alexander et al.*, 2006]. Such results have important implications at daily timescales for sectors primarily affected by either TX90pct [e.g., *Pezza et al.*, 2012] or TN90pct [e.g., *Lanning et al.*, 2011] events, where using a less suitable index (e.g.,

Table 1. Globally Averaged Trends of Each of the Five Aspects Per Index[a]

	Index	HWN	HWD	HWF	HWA	HWM
Warm Spell	TX90pct	**2.53**	**0.22**	**0.42**	**0.18**	0.05
	TN90pct	**3.39**	**0.30**	**0.54**	**0.36**	**0.19**
	EHF	**0.56**	**0.43**	**0.28**	**0.34**	0.00
Heatwave	TX90pct	**1.40**	0.08	**0.28**	0.12	0.11
	TN90pct	**1.93**	**0.14**	**0.37**	**0.20**	**0.18**
	EHF	**1.38**	**0.42**	**0.64**	**0.34**	0.00

[a]Trends are for the period 1950–2011, computed by the non-parametric Kendall slope estimator [*Sen*, 1968]. Units are percentage of monthly events per season/decade (HWN); number of days/decade (HWD); percentage of days per season/decade (HWF); °C/ for TX90pct and TN90pct, and °C^2/decade for EHF (HWA, HWM). Statistically significant trends are highlighted in bold.

TX90pct for crops sensitive to changes in T_{min}) may lead to inaccurate estimates of the impact on the sector in question.

[26] Lastly, despite different rates of change, all indices correlate well across time (see Figure 2). This is an important result since it demonstrates that while the qualitative measurements across all indices are similar, the quantitative output may differ, reinforcing the importance of selecting the appropriate metric for the impacted sector. The measurement of the 1998 El Niño in both HWD and HWA by all three indices also demonstrates the global scale impact low-frequency variability has on daily-based extreme events. El Niño-Southern Oscillation (ENSO) phases (El Niño/La Niña) may increase event duration and amplitude due to rainfall, soil moisture, and temperature changes. Previous studies have shown that extreme temperatures are affected by ENSO [e.g., *Kenyon and Hegerl*, 2008].

[27] Unfortunately, despite HadGHCND being the most comprehensive daily temperature dataset, coverage remains sparse for much of South America, Africa, and India. We therefore advise that results presented in this study are not extrapolated to regions where there are no data. Further work will employ this methodology at regional scales using different observational datasets, helping to determine the reliability of the HadGHCND dataset. Other later global studies may use observed datasets with improved coverage to understand changes in heat waves within these regions.

[28] **Acknowledgments.** The Editor thanks the two anonymous reviewers for their assistance in evaluating this paper.

References

Alexander, L. V., and J. M. Arblaster (2009), Assessing trends in observed and modelled climate extremes over Australia in relation to future projections, *Int. J. Climatol.*, *29*, 417–435, doi:10.1002/joc.1730.

Alexander, L. V., et al. (2006), Global observed changes in daily climate extremes of temperature and precipitation, *J. Geophys. Res.*, *111*, D05109, doi:10.1029/2005JD006290.

Barriopedro, D., E. M. Fischer, J. Luterbacher, R. M. Trigo, and R. García-Herrera (2011), The hot summer of 2010: Redrawing the temperature record map of Europe, *Science*, *332*, 220–224, doi:10.1126/science.1201224.

Caesar, J., L. Alexander, and R. Vose (2006), Large-scale changes in observed daily maximum and minimum temperatures: Creation and analysis of a new gridded data set, *J. Geophys. Res.*, *111*, D05101, doi:10.1029/2005JD006280.

Clark, R. T., S. J. Brown, and J. M. Murphy (2006), Modeling Northern Hemisphere summer heat extreme changes and their uncertainties using a physics ensemble of climate sensitivity experiments, *J. Clim.*, *19*, 4418–4435, doi:10.1175/JCLI3877.1.

Coumou, D., and S. Rahmstorf (2012), A decade of weather extremes, *Nat. Clim. Change*, *2*, 491–496.

Donat, M. G., and L. V. Alexander (2012), The shifting probability distribution of global daytime and night-time temperatures, *Geophys. Res. Lett.*, *39*, L14707, doi:10.1029/2012GL052459.

Fischer, E. M., and S. Shär (2010), Consistent geographical patterns of changes in high-impact European heatwaves, *Nat. Geosci.*, *3*, 398–403, doi:10.1038/ngeo866.

Fischer, E. M., D. M. Lawrence, and B. M. Sanderson (2011), Quantifying uncertainties in projections of extremes—A perturbed land surface parameter experiment, *Clim. Dyn.*, *37*, 1381–1398, doi:10.1007/s00382-010-0915-y.

Karoly, D. J. (2009), The recent bushfires and extreme heatwave in south-east Australia, *Bull. Austr. Meteorol. Oceanogr. Soc.*, *22*, 10–13.

Kenyon, J., and G. C. Hegerl (2008), Influence of modes of climate variability on global temperature extremes, *J. Clim.*, *21*, 3872–3889, doi:10.1175/2008JCLI2125.1.

Lanning, S. B., T. J. Siebenmorgen, P. A. Counce, A. A. Ambardekar, and A. Mauromoustakos (2011), Extreme nighttime air temperatures in 2010 impact rice chalkiness and milling quality, *Field Crops Res.*, *124*, 132–136, doi:10.1016/j.fcr.2011.06.012.

Meehl, G. A., and C. Tebaldi (2004), More intense, more frequent, and longer lasting heat waves in the 21st century, *Science*, *305*, 994–997, doi:10.1126/science.1098704.

Pezza, A. B., P. van Rensch, and W. Cai (2012), Severe heat waves in southern Australia: Synoptic climatology and large scale connections, *Clim. Dyn.*, *38*, 209–224, doi:10.1007/s00382-011-1016-2.

Sen, P. K. (1968), Estimates of the regression coefficient based on Kendall's tau, *J. Am. Stat. Assoc.*, *63*, 1379–1389, doi:10.1080/01621459.1968.10480934.

Trigo, R., R. Garia-Herrera, J. Diaz, I. Trigo, and M. Valente (2005), How exceptional was the early August 2003 heatwave in France?, *Geophys. Res. Lett.*, *32*, L10701, doi:10.1029/2005GL022410.

Vose, R. S., D. R. Easterling, and B. Gleason (2005), Maximum and minimum temperature trends for the globe: An update through 2004, *Geophys. Res. Lett.*, *32*, L23822, doi:10.1029/2005GL024379.

Zhang, X., et al. (2005), Trends in middle east climate extremes indices during 1950–2003, *J. Geophys. Res.*, *110*, D22104, doi:10.1029/2005JD006181.